

Effects of field-induced splitting of levels having high angular momenta

K. A. Nasyrov and A. M. Shalagin

Institute of Automation and Electrometry, Siberian Division, USSR Academy of Sciences

(Submitted 29 April 1982)

Zh. Eksp. Teor. Fiz. **83**, 1685–1697 (November 1982)

We investigate manifestations of field-induced splitting in the spectrum of a test field in the presence of a strong field resonant to an adjacent transition in a three-level system with states degenerate in the orientations of the angular momentum. We show that since the splitting effect is different for different M -transitions the spectrum of the test-field operation consists of a set of individual spectral components that can overlap at $J \gg 1$ and form a broad common spectrum. We note that the envelope of the integral spectrum includes narrow spectral structures that preserve information on the natural line width. We analyze the dependence of the shapes of the spectra on the types of transitions in a three-level system and on the polarization states of the test and strong fields. For linear and circular polarization of the strong field, the problem is solved by a rigorous quantum-mechanical approach. A classical description of the orientation of the angular momentum is used in the case of elliptic polarization of the strong field.

PACS numbers: 03.65.Db, 31.50.+w, 32.60.+i

1. INTRODUCTION

Level splitting in the field of intense resonant radiation (sometimes called the dynamic Stark effect) is one of the fundamental effects of nonlinear spectroscopy.^{1,2} It has been thoroughly studied within the framework of the model of nondegenerate states. Its strongest manifestation is the splitting of the amplification (absorption) lines of test radiation.

It is known at the same time, however, that real states of atoms and molecules are degenerate in the M -projections of the angular momentum. Since the matrix elements of the operator of the interaction with radiation are different for different M -transitions, analysis of field splitting of levels by using the model of nondegenerate states is inapplicable to real objects. In the particular cases of linear or circular polarization of the strong radiation, it has been qualitatively understood that each M -transition produces its own splitting effect; in the upshot, the spectrum of the absorption (amplification) of test radiation should contain a corresponding number of components that correspond to the individual M -transitions. However, no concrete analysis of the relative positions of these components on the frequency scale and of their relative intensities has, to our knowledge, been carried out.

Of special interest are transitions between levels with large angular momenta J . In this case the number of spectral components can be so large that they begin to overlap. This raises the question of the envelope of the spectrum, i.e., of the actual shape of the spectral line that should be observed in experiment.

Finally, if the strong radiation has an arbitrary (elliptic) polarization, even a qualitative picture of the field splitting can be obtained on the basis of the previously developed premises. Moreover, a rigorous quantum-mechanical solution of the corresponding problem is fraught with considerable mathematical difficulties. These difficulties can, however, be overcome in the case of large J by using a method^{3,4} based on the classical description of the orientation of the angular momentum.

We investigate here the effect of field-induced splitting of levels predominantly under conditions when the lines of individual M -transitions overlap. The problem is treated in one of the traditional formulations: the absorption (amplification) spectrum of test radiation is analyzed in the presence of a strong field resonant with an adjacent transition. We consider the cases of circular and linear polarization of the strong field, when a rigorous quantum-mechanical solution can be obtained, as well as the case of elliptic polarization with a classical description of the orientation of \mathbf{J} .

We show that in a sufficiently intense field the spectrum has a doublet structure and the forms of the doublet components depend significantly on the polarizations of both the strong and test fields, as well as on the ratio of the angular momenta of the combining levels. One of the salient features of the spectrum is the possible existence of narrow structures and abrupt boundaries, that preserve the information on the natural (in the absence of the strong field) line width.

The bulk of the present data on nonlinear spectroscopy (in particular, with respect to field splitting), was obtained for atomic objects. Nonlinear spectroscopy of molecules, which typically have large values of J , is now undergoing intensive development. We hope that the results of the present paper can contribute to a correct interpretation of the experimental data of nonlinear-spectroscopy experiments on molecular objects.

2. COMPONENTS OF THE SPECTRUM OF TEST RADIATION UNDER CONDITIONS OF STRONG FIELD SPLITTING

We recall first the main feature of the field splitting effect in the nondegenerate-state model. Let the strong monochromatic radiation be at resonance with the m - n transition, and the test radiation with the m - l transition (Fig. 1). In the case of homogeneous broadening, the work P_μ of the test field is described by the expression^{2,5}

$$P_\mu = 2\hbar\omega_\mu |G_\mu|^2 \operatorname{Re} \left\{ \frac{[\Gamma_{nl} - i(\Omega_\mu - \Omega)](N_l - \rho_{mm}) - iG\rho_{nm}}{[\Gamma_{nl} - i(\Omega_\mu - \Omega)][\Gamma_{ml} - i\Omega_\mu] + |G|^2} \right\} \quad (2.1)$$
$$G = Ed_{mn}/2\hbar, \quad G_\mu = E_\mu d_{ml}/2\hbar, \quad \Omega = \omega - \omega_{mn}, \quad \Omega_\mu = \omega_\mu - \omega_{ml}.$$

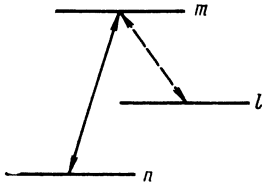


FIG. 1. Transitions in a three-level nondegenerate system.

Here E and ω are the amplitude of the electric field and the frequency of the strong radiation. The subscript μ marks the corresponding characteristics of the test radiation; Γ_{ij} are relaxation constants that characterize the broadening of the spectral line in the i - j transitions; N_i is the population of the level i in the absence of radiation.

Expression (2.1) contains the population ρ_{mm} of the level m and the off-diagonal element ρ_{mn} of the density matrix, due to the interaction with the strong field. They satisfy the equations^{2,5}

$$\begin{aligned} \rho_{mm} &= N_m + 2|G|^2 \frac{\Gamma_{mn}}{\Gamma_m} \frac{N_{nm}}{\Gamma_{mn}^2(1+\kappa) + \Omega^2}, \quad N_{nm} = N_n - N_m, \\ \rho_{nm} &= -iG^* N_{nm} \frac{\Gamma_{mn} - i\Omega}{\Gamma_{mn}^2(1+\kappa) + \Omega^2}, \quad \kappa = \frac{2|G|^2}{\Gamma_{mn}} \left(\frac{1}{\Gamma_m} + \frac{1}{\Gamma_n} \right), \end{aligned} \quad (2.2)$$

where Γ_m and Γ_n are the relaxation constants of the levels m and n . The quantity κ is the so-called saturation parameter.

The dependence of P_μ on the test-radiation frequency (on Ω_μ) is separated in explicit form in (2.1). The field-splitting effect is due entirely to the presence of the quantity $|G|^2$ in the denominator of (2.1). It manifests itself most strongly under the conditions $|G| \gg \Gamma_{nl}$, $|G| \gg \Gamma_{ml}$, and $\Omega \ll |G|$, i.e., when the strong field is intense enough. In this case it is convenient to rewrite (2.1) in the form

$$\begin{aligned} P_\mu &= 2\hbar\omega_\mu |G_\mu|^2 \operatorname{Re} \left[\frac{A_1 N_{lm} - B_1 N_{nm}}{\Gamma - i(\Omega_\mu - \Omega_1)} + \frac{A_2 N_{lm} - B_2 N_{nm}}{\Gamma - i(\Omega_\mu - \Omega_2)} \right], \\ \Gamma &= \frac{1}{2}(\Gamma_{ml} + \Gamma_{nl}), \quad \Omega_{1,2} = \frac{1}{2}(\Omega \pm [\Omega^2 + 4|G|^2]^{1/2}), \quad (2.3) \\ A_{1,2} &= \frac{\Omega_{1,2} - \Omega}{2\Omega_{1,2} - \Omega}, \quad B_{1,2} = \frac{|G|^2}{\Omega^2 + \alpha|G|^2 + \Gamma_{mn}^2} \frac{\Omega + 2\Gamma_{mn}(\Omega_{1,2} - \Omega)/\Gamma_m}{2\Omega_{1,2} - \Omega} \\ &\quad \alpha = 2\Gamma_{mn}(1/\Gamma_m + 1/\Gamma_n). \end{aligned}$$

It is distinctly seen here that the spectral line is a doublet whose components have a Lorentz shape with identical half-width and their spacing $[\Omega^2 + 4|G|^2]^{1/2}$ depends on the strong-field intensity. The ratio of the intensities of the components depends on Ω . In the important particular case $\Omega = 0$ (or $|G|^2 \gg \Omega$, which means an even higher radiation intensity) we have

$$\begin{aligned} P_\mu &= \hbar\omega_\mu |G_\mu|^2 \left[\frac{\Gamma}{\Gamma^2 + (\Omega_\mu - |G|)^2} + \frac{\Gamma}{\Gamma^2 + (\Omega_\mu + |G|)^2} \right] \\ &\quad \times \left(N_{lm} - N_{nm} \frac{\Gamma}{\Gamma_m + \Gamma_n} \right), \end{aligned} \quad (2.4)$$

i.e., the components of the doublets are of equal intensity and are symmetric about the frequency of the m - l transition. The distance between them is governed entirely by the strong field (is proportional to its amplitude).

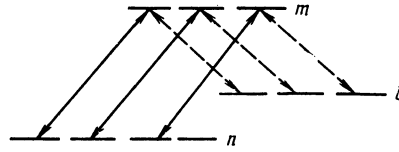


FIG. 2. The same as Fig. 1, but for degenerate states.

We consider now a situation wherein the levels m , n , and l are degenerate in the projections J_m , J_n , and J_l of the angular momenta. We assume for the sake of argument that the strong and test fields have the same linear polarization. Figure 2 shows schematically the optical transitions due to these fields. It is clearly seen from this figure that the overall system of levels and transitions breaks up into a set of three-level subsystems of the type shown in Fig. 1. Each of them can be described by the equations given above. The resultant work of the test field is given by the relation

$$P_\mu = \sum_M P_\mu(M), \quad (2.5)$$

where $P_\mu(M)$ pertains to an individual M -subsystem (M will hereafter be taken to mean the projection of the angular momentum of the level m). The results (2.1)–(2.4) remain in force for $P_\mu(M)$, provided the following substitutions are made:

$$\begin{aligned} |G|^2 &\rightarrow |G(M)|^2 = |G|^2 f(M), \\ |G_\mu|^2 &\rightarrow |G_\mu(M)|^2 = |G_\mu|^2 f_\mu(M), \\ G &= E d_{mn} / 2\hbar (2J_m + 1)^{1/2}, \quad G_\mu = E_\mu d_{ml} / 2\hbar (2J_m + 1)^{1/2}, \end{aligned} \quad (2.6)$$

where d_{mn} and d_{ml} are the reduced dipole-moment matrix elements.

It is easy to verify that subdivision into three-level subsystems is possible also when the strong radiation is circularly polarized. In either case,

$$f(M) = \frac{1}{3}(2J_m + 1) \langle J_m M J_n - M' | 1\sigma \rangle^2, \quad (2.7)$$

where σ is the polarization index ($\sigma = 0$ corresponds to linear polarization and $\sigma = \pm 1$ to circular), $\langle \dots | \dots \rangle$ is the vector-addition coefficient.

We shall analyze hereafter transitions with large level angular momenta ($J_m, J_n, J_l \gg 1$). In accord with the asymptotic values of the vector-addition coefficients,⁶ the expressions for $f(M)$ take on the form shown in Table I. If the test radiation is circularly polarized or has the same linear polarization as the strong radiation, the data in the table are valid for $f_\mu(M)$ (with allowance for the natural substitution $J_n \rightarrow J_l$). If, however, the test field has an orthogonal linear

TABLE I. Values of $f(M)$ for different types of transitions and polarizations at $J_m \gg 1$ and $J_n \gg 1$ [\uparrow denotes linear polarization, + and - denote right- and left-hand circular polarizations].

	$J_n = J_m$	$J_n = J_m - 1$	$J_n = J_m + 1$
\uparrow	M^2/J^2	$\frac{1}{2}(1 - M^2/J^2)$	$\frac{1}{2}(1 - M^2/J^2)$
$+$	$\frac{1}{2}(1 - M^2/J^2)$	$\frac{1}{4}(1 - M/J)^2$	$\frac{1}{4}(1 + M/J)^2$
$-$	$\frac{1}{2}(1 - M^2/J^2)$	$\frac{1}{4}(1 + M/J)^2$	$\frac{1}{4}(1 - M/J)^2$

polarization, $f_\mu(M)$ takes the following form:

$$f_\mu(M) = \begin{cases} 1/2(1-M^2/J^2), & J_l = J_m \\ 1/4(1+M^2/J^2), & J_l = J_m \pm 1 \end{cases} \quad (2.8)$$

We proceed now to analyze the absorption (amplification) spectrum of the test radiation. We assume that most values of M satisfy the conditions of large field splitting, i.e., $|G| \gg \Gamma_{m1}, \Gamma_{n1}$, and that Eqs. (2.3) and (2.4) hold for the individual three-level M -subsystems. We consider first the simplest case $\Omega = 0$, to which Eq. (2.4) with the substitution (2.6) corresponds. Thus, the resultant spectrum is a superposition of individual line pairs with different intensity and position in the frequency scale. According to (2.4), the distribution of the intensity among the lines is governed entirely by the function $f_\mu(M)$, i.e., it depends on the polarization of the test radiation and on the ratio of the angular momenta of the levels m and l . The positions of the lines on the frequency scale relative to the point $\Omega_\mu = 0$ are set by the value of $|G| \sqrt{f(M)}$, i.e., they are connected with the polarization and intensity of the strong field and with the ratio of J_m and J_n .

The lines are distributed in the interval between the values $\Omega_\mu = 0$ and $|\Omega_\mu| \leq |G|$ or else $|\Omega_\mu| \leq |G|/\sqrt{2}$, depending on the polarization of the strong field and on the type of the m - n transition. For linear polarization and for $\Delta_{mn} \equiv J_m - J_n = 0$, as well as for circular polarization and $\Delta_{mn} = \pm 1$, the quantity $\sqrt{f(M)}$ depends linearly on M (see Table I); the lines are therefore equidistant.

In those cases when $f(M) \propto (1 - M^2/J^2)$, the lines become strongly condensed on the edges of the spectral interval ($|\Omega_\mu| = |G|/\sqrt{2}$). This case is shown in Fig. 3.

The relative intensity of the spectral components is unevenly distributed in all cases. In accordance with the different $f_\mu(M)$ for the different polarization states of the test field and different types of the m - l transition, a greater weight is possessed either by components located closer to the line center (see Fig. 3a) or by those farthest from it (Fig. 3b).

At $\Omega \neq 0$ the spectrum components described by (2.3) become asymmetric about the point $\Omega_\mu = 0$. Their intensities are now determined not only by $f_\mu(M)$ but also by the function $f(M)$ connected with the strong field. The positions of the components on the frequency scale are governed as before only by the characteristics of the strong field and of

the m - n transition. The qualitative results for $\Omega_\mu = 0$ remain in force also for $\Omega \neq 0$. Their main consequence is that both the distribution of the components over the spectrum and their relative intensities have an exceedingly strong dependence on the field polarizations and on the relations between J_m, J_n , and J_l . As a consequence, the form of the resultant spectrum undergoes appreciable modifications.

3. SHAPE OF THE PRINCIPAL PART OF THE SPECTRUM ENVELOPE

We assume that the natural width of the radiation line ensures overlap of the individual M -components of the spectrum. Then, in analogy with the known inhomogeneous-broadening situation, the resultant spectrum is described by a relatively smooth envelope. If the number of components is large enough ($J_m, J_n, J_l \gg 1$), the summation over M in (2.5) can be replaced by integration. In the case of strong field splitting an integrand of the form (2.3) contains a "peaked" function of M with smoothly varying parameters. Taking this circumstance into account and putting formally $\Gamma \rightarrow 0$ we can obtain the integration results in the form

$$P_\mu = D \sum_{y_0} |G_\mu(y_0)|^2 / |d/dy| G(y)|^2 |_{y=y_0}, \quad y = M/J, \quad (3.1)$$

$$D = \pi \hbar \omega_\mu$$

$$\times \left[N_{lm} |\Omega_\mu - \Omega| - N_{nm} \frac{\Omega_\mu (\Omega_\mu - \Omega) |2(\Gamma_{mn}/\Gamma_m)(\Omega_\mu - \Omega) + \Omega|}{\Gamma_{mn}^2 + \Omega^2 + \alpha \Omega_\mu (\Omega_\mu - \Omega)} \right]$$

Here N_{lm} and N_{nm} are the total population differences of the corresponding levels in the absence of radiation. The summation in (3.1) is over those values of y_0 for which the inequality

$$|G(y_0)|^2 = \Omega_\mu (\Omega_\mu - \Omega) = u \quad (3.2)$$

is satisfied. This relation specifies, in particular, the spectral-region boundaries in which P_μ differs substantially from zero. There are two such regions:

$$1/2 \{ \Omega - [\Omega^2 + 4|G(y_0)|_{max}^2]^{1/2} \} \leq \Omega_\mu \leq 0, \quad (3.3)$$

$$\Omega \leq \Omega_\mu \leq 1/2 \{ \Omega + [\Omega^2 + 4|G(y_0)|_{max}^2]^{1/2} \}.$$

Thus the envelope of the spectrum is also a doublet, but its components are to a certain degree "inhomogeneously" broadened.

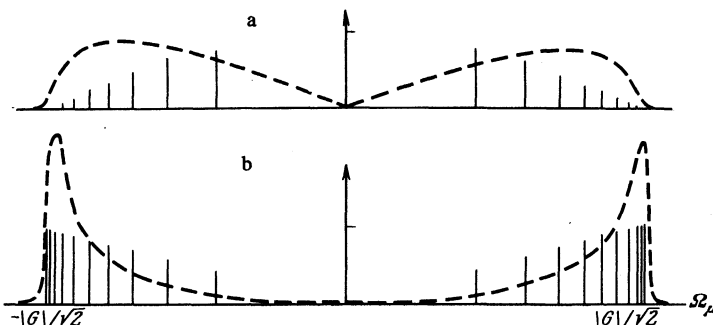


FIG. 3. Distribution in frequency and relative intensity of the spectral components at $J_m = 10, J_n = 11, J_l = 10$, and $\Omega = 0$; a) || (parallel polarizations of the strong and test fields); b) ⊥ (perpendicular polarizations of the fields).

We present for P_μ a summary of the formulas, which corresponds to expression (3.1) under different polarization conditions and for different types of transitions.

$$P_\mu = D(|G_\mu|^2/|G|^2)\varphi_\mu, \quad \Delta_{mn} \equiv J_m - J_n, \quad \Delta_{ml} \equiv J_m - J_l;$$

for $\Delta_{mn} = 0$ and $\Delta_{ml} = 0$ we have

$$\varphi_\mu = \begin{cases} (u/|G|^2)^{1/2}, & \parallel \\ 1/2(1-u/|G|^2)/(u/|G|^2)^{1/2}, & \perp \\ 2u/|G|^2(1-2u/|G|^2)^{1/2}, & + \end{cases}, \quad 0 \leq u \leq |G|^2, \quad (3.4)$$

for $\Delta_{mn} = 0$ and $\Delta_{ml} = \pm 1$

$$\varphi_\mu = \begin{cases} 1/2(1-u/|G|^2)/(u/|G|^2)^{1/2}, & \parallel \\ 1/4(1+u/|G|^2)/(u/|G|^2)^{1/2}, & \perp \\ (1-u/|G|^2)/(1-2u/|G|^2)^{1/2}, & + \end{cases}, \quad 0 \leq u \leq |G|^2/2, \quad (3.5)$$

for $\Delta_{mn} = \pm 1$ and $\Delta_{ml} = 0$

$$\varphi_\mu = \begin{cases} 2(1-2u/|G|^2)^{1/2}, & \parallel \\ 2u/|G|^2(1-2u/|G|^2)^{1/2}, & \perp \\ 2(1-u^{1/2}/|G|), & + \end{cases}, \quad 0 \leq u \leq |G|^2, \quad (3.6)$$

and for $\Delta_{mn} = 1$ and $\Delta_{ml} = \pm 1$

$$\varphi_\mu = \begin{cases} 2u/|G|^2(1-2u/|G|^2)^{1/2}, & \parallel \\ (1-u/|G|^2)/(1-2u/|G|^2)^{1/2}, & \perp \\ \frac{|G|}{u^{1/2}} \left[\frac{u}{|G|^2} \left| \frac{G_{\pm 1}^\mu}{G^\mu} \right|^2 + \left(1 - \frac{u^{1/2}}{|G|}\right)^2 \left| \frac{G_{\mp 1}^\mu}{G^\mu} \right|^2 \right], & + \end{cases}, \quad 0 \leq u \leq |G|^2. \quad (3.7)$$

We have used here the symbol $u = \Omega_\mu(\Omega_\mu - \Omega)$. The + sign corresponds to circular polarization of the strong field. In all cases, with exception of the transitions $|\Delta_{mn}| = |\Delta_{ml}| = 1$, the value of P_μ does not depend on the polarization of the test field.

Typical forms of the spectrum at $\Omega = 0$ are shown in Fig. 4. The spectrum is symmetrical about the point $\Omega_\mu = 0$ and has in many cases a doublet structure. The latter is absent in four cases, when the function φ_μ in (3.4)–(3.7) is proportional to $u^{-1/2}$ (see also Figs. 4c and 4h). The spectrum boundaries correspond to the maximum splitting effect for individual M -components and is located at $|\Omega_\mu| = |G|$ or at $|\Omega_\mu| = |G|/\sqrt{2}$. Figures 4e and 4f show that the field splitting effect can be quite pronounced even in the envelope of the spectrum, provided definite polarization conditions are satisfied. In this case P_μ is proportional to $(1-2u/|G|^2)^{-1/2} = (1-2\Omega_\mu^2/|G|^2)^{-1/2}$, which indicates a rapid growth of P_μ when $|\Omega_\mu|$ approaches the edges of the contour, or even a divergence. The increase of the intensity on the edges of the contour is due to condensation of the M -components of the spectrum (see Fig. 3 and its discussion). Divergence, on the other hand, sets in when Γ is neglected. The behavior of the spectrum at the edges of the spectrum will be detailed below.

We note that in all cases the area of the contours on Fig. 4 is the same. The reason is that the area of the contour of each individual M component (the integral of expression

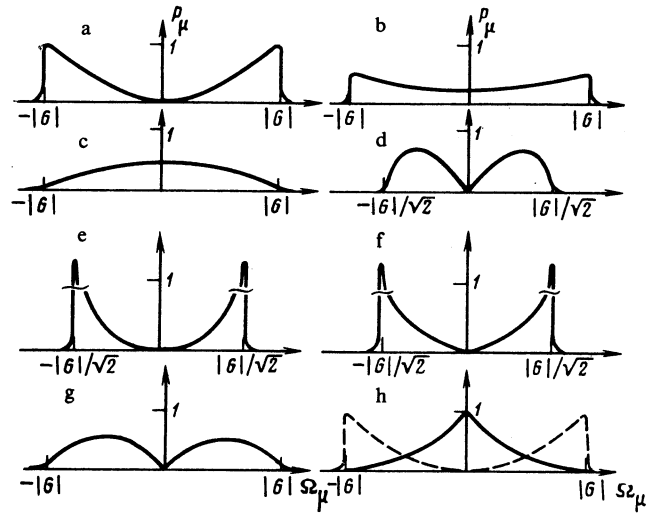


FIG. 4. Spectra at $\Omega = 0$ in the scale $(\pi\Gamma_\mu|G_\mu|^2/|G|)[(N_{lm} - N_{nm}\Gamma_n)/(\Gamma_n + \Gamma_m)]$: a) $\Delta_{mn} = 0, \Delta_{ml} = 0, \parallel$; b) $\Delta_{mn} = 0, \Delta_{ml} = 1, \perp$; c) $\Delta_{mn} = 0, \Delta_{ml} = 0, \perp$; $\Delta_{mn} = 0, \Delta_{ml} = 1, \parallel$; d) $\Delta_{mn} = 1, \Delta_{ml} = 0, \parallel$; e) $\Delta_{mn} = \Delta_{ml} = 1, \parallel$; $\Delta_{mn} = 1, \Delta_{ml} = 0, \perp$; $\Delta_{mn} = \Delta_{ml} = 0, +$; f) $\Delta_{mn} = \Delta_{ml} = 1, \perp$; $\Delta_{mn} = 0, \Delta_{ml} = 1, +$; g) $\Delta_{mn} = 1, \Delta_{ml} = 0, +$; h) $\Delta_{mn} = \Delta_{ml} = 1, +$; the solid and dashed lines show the contours for coinciding and orthogonal polarizations of the test field, respectively.

(2.4) for $P_\mu(M)$ with respect to Ω_μ) is determined only by the value of $|G_\mu(M)|^2$. Therefore the area of the integral contour depends in turn, by virtue of the properties of the Clebsch-Gordon coefficients, only on $|G_\mu|^2$, i.e., on the intensity but not on the polarization state of the test field.

We consider now the more general case $\Omega \neq 0$. We note that at $\Omega \neq 0$ the terms proportional to N_{lm} and N_{nm} have substantially different frequency dependences and they must be considered separately. We agree to assign a plus sign to the first term ($N_{lm} > 0$) and a minus sign to the second ($N_{nm} > 0$). The corresponding spectra calculated from Eqs.

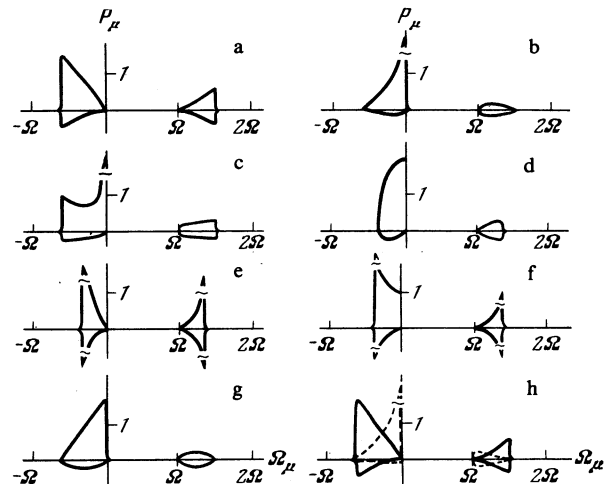


FIG. 5. Spectra at $\Omega \neq 0$ in the scale $\pi\Gamma_\mu|G_\mu|^2/|G|$; $P_\mu > 0$ pertains to the case $N_{lm} = 1, N_{nm} = 0$, while $P_\mu < 0$ to the case $N_{lm} = 0, N_{nm} = 1$: a) $\Delta_{mn} = \Delta_{ml} = 0, \parallel$; b) $\Delta_{mn} = \Delta_{ml} = 0, \perp$; $\Delta_{mn} = 0, \Delta_{ml} = 1, \parallel$; c) $\Delta_{mn} = 0, \Delta_{ml} = 1, \perp$; d) $\Delta_{mn} = 1, \Delta_{ml} = 0, \parallel$; e) $\Delta_{mn} = 1, \Delta_{ml} = 0, \perp$; $\Delta_{mn} = \Delta_{ml} = 0, +$; f) $\Delta_{mn} = \Delta_{ml} = 1, \perp$; $\Delta_{mn} = 0, \Delta_{ml} = 1, +$; g) $\Delta_{mn} = 1, \Delta_{ml} = 0, +$; h) $\Delta_{mn} = \Delta_{ml} = 1, +$; the solid and dashed lines show the contours for coinciding the orthogonal polarizations of the test field.

(3.4)–(3.7) are shown in Fig. 5. As can be seen from the figure, the absorption (amplification) spectrum of the test field always has the form of a doublet at $\Omega \neq 0$. The spectral intervals are set by the conditions (3.3). The doublet components differ not only in intensity but can also have entirely different shapes. Just as at $\Omega = 0$, in some cases the edges of the lines take the form of sharp peaks. Their presence is also due to condensation of the M components.

4. BOUNDARY REGIONS AND LINE WINGS

Equations (3.4)–(3.7), which are based on the approximation (3.1), describe sufficiently well only the internal part of the doublet line. They no longer hold near the edges (we have already seen that they lead even to divergences). It is typical that the inner and outer edges ($\Omega \neq 0$) should be described differently. Indeed, the contributions to the inner edges ($\Omega_\mu \approx 0, \Omega_\mu \approx \Omega$) come from M -transitions with small values of $|G(M)|$ [see condition (3.2)], and the approximate formula (2.3) must be made more precise here. For the outer edges, Eq. (2.3) remains valid, it is only necessary to use a correct value of Γ . In both cases, the amplitudes of the M -components at the contour edges are important. If they differ from zero, the transition from the main part of the contour to its wings is effected in the following manner.

In those cases when a divergence appears in Eqs. (3.4)–(3.7), i.e., in the expressions containing $u^{-1/2}$ and $(1 - 2u/|G|^2)^{-1/2}$, the following substitutions must be made in the vicinity of the singular points:

$$|G|u^{-1/2} \rightarrow g(\Delta\Omega_\mu), \quad (1 - 2u/|G|^2)^{-1/2} \rightarrow g(-\Delta\Omega_\mu),$$

$$g(\Delta\Omega_\mu) = \frac{1}{\sqrt{2}} \frac{\Gamma|G|}{(\Gamma^2 + \Delta\Omega_\mu^2)^{1/2}} [(\Gamma^2 + \Delta\Omega_\mu^2)^{1/2} - \Delta\Omega_\mu]^{-1/2} \times |2\Omega_\mu^0 - \Omega|^{-1/2}, \quad (4.1)$$

$$\Delta\Omega_\mu = (\Omega_\mu - \Omega_\mu^0) \cdot \text{sgn}(2\Omega_\mu^0 - \Omega).$$

To simplify matters we have put here $\Gamma_{ml} = \Gamma_{nl} = \Gamma$; the frequency Ω_μ^0 is the position of the singular point (the corresponding end point of the spectral line). In the first case $\Omega_\mu^0 = 0$, i.e., the singular point can be only at $\Omega_\mu = 0$ (see Fig. 5). In the second case there are two such points, $\Omega_\mu^0 = \frac{1}{2}[\Omega \pm (\Omega^2 + 2|G|^2)^{1/2}]$.

If the quantity P_μ calculated from Eqs. (3.4)–(3.7) has on the line boundary a finite nonzero value P_μ^0 , the corrected behavior of P_μ near the boundary (Ω_μ^0) is described by the equations

$$P_\mu = P_\mu^0 h(\Delta\Omega_\mu), \quad \Omega_\mu^0 = 0, \quad (4.2)$$

$$P_\mu = P_\mu^0 h(-\Delta\Omega_\mu), \quad \Omega_\mu^0 = \frac{1}{2}[\Omega \pm (\Omega^2 + 4|G|^2)^{1/2}],$$

where

$$h(\Delta\Omega_\mu) = \frac{1}{2} + \pi^{-1} \text{arctg}(\Delta\Omega_\mu/\Gamma).$$

The characteristic scale of the variation of the functions $g(x)$ and $h(x)$ is the natural line width Γ . Since we assume Γ to be small compared with the total width of each of the doublet components, the line shape is completely described by these functions in the vicinity of the boundaries.

At $\Delta\Omega_\mu = 0$ we have $g(0) = |G|(2\Gamma|2\Omega_\mu^0 - \Omega|)^{-1/2}$. This quantity is finite, in contrast to the results of the preced-

ing description, but its value is larger the smaller Γ . For $h(\Delta\Omega_\mu)$ at the point $\Omega_\mu = \Omega_\mu^0$ we have $h(0) = \frac{1}{2}$. This means that $P_\mu(\Omega_\mu^0) = P_\mu^0/2$, or half the limiting value obtained from the corresponding formulas (3.4)–(3.7).

The asymptotic values of $g(x)$ and $h(x)$ at $|x| \gg \Gamma$ are

$$g(x) = |G|(x|2\Omega_\mu^0 - \Omega|)^{-1/2}, \quad h(x) = 1 \quad (x > 0),$$

$$g(x) = \frac{1}{2}\Gamma|G||x|^{-3/2}|2\Omega_\mu^0 - \Omega|^{-1/2}, \quad h(x) = \pi^{-1}\Gamma/|x| \quad (x < 0). \quad (4.3)$$

It is easy to verify on the basis of this result that following a shift within the spectral line ($x > 0$) Eqs. (4.1) and (4.2) are correctly “matched” to the corresponding Eqs. (3.1)–(3.7). Corresponding to the opposite asymptotic behavior ($x < 0$) are the line wings. The function $g(x)$ ensures more rapidly decreasing wings $\propto |\Delta\Omega_\mu|^{-3/2}$ than does the function $h(x)$, where the wings $\propto |\Delta\Omega_\mu|^{-1}$. This is understandable, for in the former case the M -components of the spectra condense near the boundary. It is they which make the main contribution to the wings.

The edges of the lines near which P_μ calculated from Eqs. (3.4)–(3.7) vanishes are described by rather unwieldy expressions which will not be given here. We note only that these spectral intervals receive comparable contributions from all the M -components of the corresponding doublet component. For this reason the line wing also decreases quite slowly (slower than $|\Delta\Omega_\mu|^{-1}$).

If $\Omega = 0$ and there is no doublet splitting of the line (Figs. 4b, 4c, 4h), the region of $\Omega_\mu = 0$ calls for a special analysis. Indeed, this spectral region is formed by M -components for which the field splitting is small ($|G(M)|$ is smaller than or comparable with the relaxation constants). Consequently the approximate formula (2.3) is not applicable here. On the other hand, it is known² that at relatively small $|G|$ the absorption (amplification) line of the test field depends significantly on the ratio of the relaxation constants. The behavior of the spectrum envelope of the spectrum in the vicinity of $\Omega_\mu = 0$ with interval $|\Omega_\mu| \propto \tilde{\Gamma}$ (where $\tilde{\Gamma}$ is the effective relaxation constant) is thus expected to differ from the limiting values obtained from (3.4)–(3.7). Indeed, a computer calculation has shown that singularities in the form of a peak or of a dip can indeed be observed in the vicinity of $\Omega_\mu = 0$ (see Fig. 6). The widths of these structures are of the order of the natural line widths, i.e., of the order of Γ .

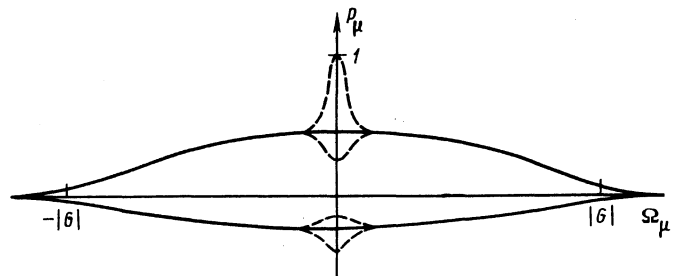


FIG. 6

5. ELLIPTIC POLARIZATION OF STRONG FIELD

The rigorous quantum-mechanical solution of the problem becomes exceedingly more complicated if the strong field is elliptically polarized. At large value of the quantum numbers J_m, J_n, m and J_l , however, a classical description of the orientation of the angular momenta is found to be effective.^{3,4} In other words, one introduces the elements of the density matrix $\rho_{ij}(\mathbf{s})$ ($i, j = m, n, l$), where \mathbf{s} is a unit vector in the angular-momentum direction. As shown in Ref. 4, $\rho_{ij}(\mathbf{s})$ satisfies exactly the same equations as the elements ρ_{ij} in the model of nondegenerate states. The only formal difference lies in the additional (parametric) dependence of ρ_{ij} on \mathbf{s} . This dependence is due to the $G(\mathbf{s})$ and $G_\mu(\mathbf{s})$ dependences, for which the following equations are valid⁴

$$G(\mathbf{s}) = \sum_{\sigma} G_{\sigma} D_{\sigma \Delta_{mn}}^{1*}(\varphi, \theta, 0), \quad G_{\sigma} = E_{\sigma} d_{mn} / 2\hbar (2J+1)^{1/2}, \quad (5.1)$$

$$G_{\mu}(\mathbf{s}) = \sum_{\sigma} G_{\sigma}^{\mu} D_{\sigma \Delta_{ml}}^{1*}(\varphi, \theta, 0), \quad G_{\sigma}^{\mu} = E_{\sigma}^{\mu} d_{ml} / 2\hbar (2J+1)^{1/2}.$$

Here E_{σ} and E_{σ}^{μ} are the circular components of the electric vectors of the fields; φ and θ are the azimuthal and polar angles of the vector \mathbf{s} , and $D_{\sigma \Delta}^1$ is the Wigner rotation matrix.

The work of the test field is given by the natural expression

$$P_{\mu} = \frac{J}{2\pi} \int P_{\mu}(\mathbf{s}) d\mathbf{s}, \quad (5.2)$$

where Eq. (2.1) remains valid for $P_{\mu}(\mathbf{s})$, recognizing that now G and G_{μ} depend on \mathbf{s} in accordance with (5.1).

The summation over the discrete variable in (2.5) is replaced in (5.2) by integration. This means that the line contour described by (5.2) is directly a smooth envelope. It is clear therefore that from the viewpoint of the problem considered the classical description of the angular-momentum orientation contains automatically the assumption that neighboring elements of the spectrum components overlap. If it is assumed that $P_{\mu}(\mathbf{s})$ does not depend on the angle θ and it is recognized that $\cos \theta = M/J$, then Eq. (5.2) is a transition from summation in (2.5) to integration.

We shall assume that the condition $|G(\mathbf{s})| \gg \Gamma_{ml}, \Gamma_{nl}$ is satisfied in the entire range of variation of θ and φ . It is then possible to use the approximation (2.3) and, in addition, integrate explicitly in (5.2) with respect to one of the variables (say, θ). We then obtain (cf. (3.1))

$$P_{\mu} = \frac{D}{2\pi} \int_0^{2\pi} \sum_{y_0} |G_{\mu}(y_0, \varphi)|^2 / \left| \frac{d}{dy} |G(y, \varphi)|^2 \right|_{y=y_0} d\varphi, \quad (5.3)$$

$$y = \cos \theta, \quad G_{\mu}(y, \varphi) \equiv G_{\mu}(\mathbf{s}), \quad G(y, \varphi) \equiv G(\mathbf{s}),$$

where the summation is over values of y_0 satisfying the equation

$$|G(y_0, \varphi)|^2 = \Omega_{\mu}(\Omega_{\mu} - \Omega). \quad (5.4)$$

The factor D is described by Eq. (3.1) as before.

Subject to the conditions under which the problem was solved in the preceding sections, we can choose a coordinate

frame in which the functions $G_{\mu}(y, \varphi)$ and $G(y, \varphi)$ do not depend on φ . In this case, as should be the case, Eq. (5.3) coincides with (3.1).

It will be more convenient in the analysis that follows to integrate in (5.2) first with respect to the angle φ . In the coordinate system where the propagation directions of the strong and test waves coincides with the z axis we obtain

$$P_{\mu} = \frac{D}{\pi} \int_0^{2\pi} d\theta \sin \theta \left\{ G_{+1}^{\mu^2}(\theta) + G_{-1}^{\mu^2}(\theta) + \cos 2(\psi^{\mu} - \psi) \right. \\ \times \frac{G_{+1}^{\mu}(\theta) G_{-1}^{\mu}(\theta)}{G_{+1}(\theta) G_{-1}(\theta)} (u - G_{+1}^2(\theta) - G_{-1}^2(\theta)) \left. \right\} \\ \times \{ [|G_{+1}(\theta)| + |G_{-1}(\theta)|]^2 - u \} \\ \times [u - (|G_{+1}(\theta)| - |G_{-1}(\theta)|)^2]^{-1/2}, \quad (5.5)$$

$$G_{\sigma}(\theta) = |G_{\sigma}| d_{\sigma \Delta_{mn}}^1(\theta), \quad G_{\sigma}^{\mu}(\theta) = |G_{\sigma}^{\mu}| d_{\sigma \Delta_{ml}}^1(\theta), \quad \sigma = \pm 1,$$

$$u = \Omega_{\mu}(\Omega_{\mu} - \Omega),$$

ψ^{μ} and ψ are the orientation angles of the polarization ellipses of the test and strong fields.

In the particular cases when the strong field is linearly or circularly polarized, we easily obtain from (5.5), taking the limits $|G_{-1}| \rightarrow |G_{+1}|$ and $|G_{-1}| \rightarrow 0$ the previously derived expressions (3.4)–(3.7) for the work of the test field. If the strong field is elliptically polarized, the integral (5.5) cannot be evaluated in terms of elementary functions, and it is necessary to resort to numerical methods. A very simple analysis shows nevertheless that at certain values of u the integral (5.5) diverges logarithmically. The singular values u^0 are determined from the conditions

$$R(\cos \theta) = 0, \quad dR/d \cos \theta = 0, \quad d^2R/d \cos^2 \theta > 0,$$

where R is the radicand in the integral (5.5). It follows hence that sharp peaks can appear at the singular points of the spectrum $u^0 = \frac{1}{2}(|G_{+1}| - |G_{-1}|)^2$ for the $J_m = J_n$ transition and $u^0 = |G_{-1}|^2$ for $J_m = J_n \pm 1$ (we put for the sake of argument $|G_{+1}| > |G_{-1}|$). These peaks can appear or vanish, depending on the type of the $m-l$ transition and on the polarization of the test field. For example, at any polarization of the test field these peaks are always present in the spectrum of a three-level system for the transitions $|\Delta_{mn}| = 1$ and $|\Delta_{ml}| = 1$, and are always absent for $|\Delta_{mn}| = 1$ and $\Delta_{ml} = 0$. If the test field is chosen to have a linear polarization oriented along the major axis of the strong-field polarization el-

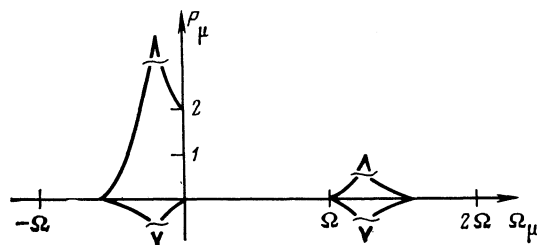


FIG. 7. Spectrum for $\Delta_{mn} = 0, \Delta_{ml} = 1$, and test-field linear polarization oriented along the major axis of the strong-field polarization ellipse.

lipse, a sharp maximum will be observed within the line doublets at $D_{mn} = 0$ and $|\Delta_{ml}| = 1$, and will be absent for the transitions $\Delta_{mn} = 0$ and $\Delta_{ml} = 0$. The situation is reversed if the test field has a polarization perpendicular to the strong-field polarization-ellipse orientation. Figure 7 shows the line contour for the transitions $\Delta_{mn} = 0$ and $|\Delta_{ml}| = 1$ when the test-field linear polarization is oriented along the strong-field polarization-ellipse major axis. In contrast to the cases of linear and circular polarizations of the strong field (see Figs. 5b and 5f), an abrupt increase of the intensity is observed here not at the ends of the lines, but in the internal regions. Consequently, when the strong-field polarization is smoothly varied from linear to circular, a smooth displacement of the sharp peak should be observed from one edge of the doublet component to the other.

6. CONCLUSION

The analysis in the present paper shows that in systems with large rotational quantum numbers the field splitting of the levels manifests itself quite unusually. First, the components of the known doublet are subject to a strong "inhomogeneous" broadening. Sometimes the doublet structure disappears completely. In the cases when it is preserved, each of the components is represented by an envelope that occupies a spectral region that exceeds considerably the natural line width.

The shape of the doublet components depends very strongly on the polarization conditions and on the type of transition. In some cases the intensity increases sharply on the edges or in the internal parts of the lines. The characteristic scale of the corresponding peaks is governed by the value of Γ .

Despite the large broadening of the components, the spectrum retains information on the natural width. Besides the already noted peak width, this information is contained in the abrupt edges of the lines. In addition, in some cases (at $\Omega = 0$) in the vicinity of the spectral line ($\Omega_{\mu} = 0$) additional peaks or dips can arise having a natural width and amplitude that depends on the ratio of the relaxation constants.

To be able to observe the considered effects in experiment, for example in vibrational-rotational transitions of molecules, the following conditions must be satisfied. First, the absorption line must be sufficiently isolated, i.e., the distance to the other lines should exceed substantially the natural (in most cases, Doppler) width. Second, the resonant-radiation intensity must be high enough to cause field splitting on individual M -components; the splitting must exceed the Doppler width, but not be high enough to excite higher vibrational states. These conditions can be satisfied for a large class of relatively simple molecules, at least for almost all diatomic molecules. To be specific, we present the following estimates for HF, a typical working gas in chemical lasers. The rotational constant for HF is $\sim 6 \times 10^{11}$ Hz, and the line shift due to anharmonicity is $\sim 3 \times 10^{12}$ Hz (Ref. 7). Recognizing that the Doppler width for the vibrational transitions of HF is $\sim 10^8$ Hz, we verify that the absorption spectrum of HF is very sparse. Using the data of Ref. 8 on the value of the Einstein coefficient A for an individual vibrational-rotational transition of HF ($A \sim 2 \times 10^2 \text{ sec}^{-1}$), we find that the field splitting exceeds by 10 times the Doppler width at a radiation intensity $\sim 10^7 \text{ W/cm}^2$. This by far not the record value of the HF laser radiation intensity.

¹V. S. Letokhov and V. P. Chebotaev, *Nonlinear Laser Spectroscopy*, Springer, 1977.

²S. G. Rautian, G. I. Smirnov, and A. M. Shalagin, *Nelineinye rezonansy v spektrakh atomov i molekul (Nonlinear Resonances in the Spectra of Atoms and Molecules)*, Novosibirsk, Nauka, 1979.

³M. Ducloy, *J. Phys.* **B9**, 357 (1976).

⁴K. A. Nasyrov and A. M. Shalagin, *Zh. Eksp. Teor. Fiz.* **81**, 1649 (1981) [*Sov. Phys. JETP* **54**, 877 (1981)].

⁵t. Ya. Popova, A. K. Popov, S. G. Rautian, and R. I. Sokolovskii, *Zh. Eksp. Teor. Fiz.* **57**, 850 (1969) [*Sov. Phys. JETP* **30**, 466 (1970)].

⁶D. A. Varshalovich, A. N. Moskalev, and V. K. Khersonskii, *Kvantovaya teoriya uglovogo momenta (Quantum Theory of Angular Momentum)*, Nauka, 1975.

⁷G. Herzberg, *Diatomic Molecules*, Van Nostrand, 1951.

⁸G. Emanuel, H. Cohen, and T. A. Jacobs, *J. Quant. Spectr. Rad. Trans.* **13**, 1365 (1973).

Translated by J. G. Adashko